On the solutal and thermal Marangoni convection arising in the self-rewetting fluid flow under hydromagnetic consideration

Vineet Kumar Chaurasiya, Rajat Tripathi* and Ramayan Singh.

Department of Mathematics, National Institute of Technology, Jamshedpur-831014, Jharkhand, India

Corresponding author: Mob: +91 7909067450

Email addresses: 1990.vineet.1990@gmail.com, (V.K.Chaurasiya);

rtripathi.math@nitjsr.ac.in; (R.Tripathi);

rsingh.math@nitjsr.ac.in (R. Singh)

Abstract:

In the present research article, we address the magnetically controlled thermal and solutal Marangoni convection in the flow of self-rewetting power-law liquid over a disk, in the existence of a space dependent heat source. The self re-wetting property of fluid is modelled by considering a quadratic dependence of surface tension on temperature and species concentration. The aforementioned problem is modelled by simplified Navier-Stokes equations. Identifying the appropriate transform variables is essential for developing ordinary differential equations from original partial differential equations that describe the flow conditions. The resulting ordinary differential equations are solved by using the *bvp4c* routine of MATLAB and numerical solutions are presented via Graphs and tables, illustrating the impact of several factors on fluid velocity, temperature, and concentration. Computation of the quantities of physical interest such as Nusselt and Sherwood numbers are also done from those numerical solutions. One of the key findings of present research work is that the Marangoni convection works differently for pseudo-plastic fluid and dilatant fluid. On increasing thermal Marangoni convection the temperature of dilatant fluid reaches a peak value much closer to the disk than temperature of pseudo plastic fluid.

Keywords: Marangoni convection; Magnetic field; Space dependent heat source; Power-law fluid; self-rewetting fluid;

1 Introduction

Non-Newtonian fluids are widely used in industry and science, including microfluidic devices, oil recovery and blood rheology, among others. Because of the nonlinear dependence of shear stress with shear strain Sahu et al. [1], these fluids are more difficult to model than Newtonian fluids. Non-Newtonian fluids are classified into several categories and there are different models depicting their behaviour. This has been duly noted and explained in the works of Kumar et al. [2], Hussain and Jamshed [3] and Kumar et al. [4]. Power law fluid is one such fluid model. It is based on the viscosity model for time-independent coefficient of viscosity and can be used to model various fluids

used in industrial applications. The magnitude of the power-law index determines the physical trait of the fluid; it may behave like shear-thinning (pseudo-plastic), Newtonian or shear-thickening (dilatant) fluid Wang and Yu [5]. The rheological equation of state for a power-law fluid is given as

$$\tau_r = K \left| \frac{\partial U}{\partial Z} \right|^{n-1} \frac{\partial U}{\partial Z},$$

in which K denotes flow consistency index and $\frac{\partial U}{\partial Z}$ gives shear rate normal to the plane of shear. The fluid is classified as Newtonian for power-law index $n = 1$, a pseudoplastic when $n \epsilon (0, 1)$, and a Dilatant fluid for $n > 1$. In recent past, a lot of studies were done to investigate power-law fluid flow under various conditions. Nitin and Chhabra [6] considered the axi-symmetric two-dimensional power-law fluid moving past a circular surface. The heat transport analysis for the flow of an incompressible power-law fluid with forced convection over a heated elliptical cylinder was done by Bharti et al. [7]. Ming et al. [8] discussed the flow of a power-law liquid over an infinite rotating disk about the transverse direction. Li et al. [9] in their study considered different thermal conductivity models in their investigation of two-dimensional power law fluid flow in a circular duct. Li and Jiang [10] investigated two different models of thermophoresis and Brownian diffusion effects on Newtonian and non-Newtonian fluid flow in a rotating groove. Gaffar et al. [11] considered effect of the buoyancy on third grade fluid flowing over cylinder by considering the fluid to be radiative, using Keller-Box technique. Sadiq and Hayat [12] investigated the three-dimensional incompressible flow of a non-Newtonian Reiner-Rivlin fluid flowing over a shrinking/streching rotating circular surface with thermophoresis, Brownian and random diffusion effects.

The Marangoni convection may occur at a fluid-fluid interface when there is a gradient in the interfacial tension. As a result, fluid movement is observed from regions with smaller interfacial tension toward those with higher interfacial tension. The thermal Marangoni convection (also known as thermocapillary convection) and/or solutal Marangoni convection appears when surface tension relies on the thermal and/or concentration distributions. In last few decades, many researchers have studied the flow due to Marangoni convection owing to their vast occurance in natural as well as industrial phenomena such as tear of wines, evaporation-condensation cycle in heat pipes, controlled Marangoni convection in crystal growth, etc. Also, Marangoni convection affects a wide range of processes occurring at a nonisothermal interface. Napolitano [13] discussed the buoyancy as well as Marangoni convection at the interface of two immiscible fluid and performed an order of magnitude analysis to ascertain different flow regime for natural and Marangoni convection. Boeck and Thess [14] examined the two-dimensional thermocapillary convection on the free surface with high value of the Prandtl number. Lin and Zheng [15] discussed the Marangoni convection in the Cu-based nanofluid flowing over a porous disk. Gupta and Surya [16] considered Benard-Marangoni convection on flow of thin liquid film with linear surface tension. In a

Maxwell power-law fluid flow, Kumari and Tripathi [17] examined the irreversibility analysis of thermo-solutal Marangoni convection.

As discussed above, the presence of solutal and thermal gradients induce Marangoni convection. However, a controlled Marangoni convection is required in some engineering application such as coating of chemical on semiconductor substrate. Also, while growing perfect crystals in space-ships, sometimes uncontrolled Marangoni convection results in the crystal of substandard quality. It has been pointed out that controlled Marangoni convection can be achieved by applying a suitable magnetic field Jin et al. [18]. Such requirement in the past encouraged researchers to investigate the Marangoni convection when the flow region is influenced by magnetic field. Wilson [19] numerically determined the influence of Marangoni convection as well as magnetic field in horizontal layer of a fluid flowing over a rigid lower surface when heat flux is already prescribed. Magyari and Chamkha [20] found exact solution of Magneto-Marangoni convection and elaborated their simultaneous influences on heat transfer. Abel et al. [21] contemplated the hydromagnetic treatment of stagnation point flow of a fluid governed by power law. Jiao et al. [22] discussed Magnetohydrodynamic flow of a fluid regulated by power law, past a surface by considering Marangoni convection due to concentration and thermal gradients under Magnetohydrodynamic effects. Jawad et al. [23] analysed thermo-capillary convection of Maxwell power-law nano liquid flowing over an elongating surface while considering the heat dissipation produced by magnetic field. Nandi and Kumbhakar [24] analyzed the flow of tangent hyperbolic nanofluid flowing over a wedge under Hydromagnetic assumptions. Tripathi [25] discussed the flow of hybrid nano-liquid past an elongating disk by considering the effect of Marangoni convection. He found that the use of blade-shaped nano particles in hybrid nano-liquid result in maximum heat transfer at the disk surface. Hussain [26] carried out the quadratic regression approximation analysis for heat transport rate and flow parameters of nanofluids. The significance of heat generation/absorption, magnetic and other parameters results are shown graphically. Maxwell fluid flow with a thermal slip under the influence of Soret-Dufour and second-order nonlinear stretching slips due to the presence of magnetic field were examined by Abbas et al. [27].

Liquids generally exhibit a decrement in surface tension when temperature is increased. But self re-wetting fluids have the property that with an increase in temperature, initially surface tension decreases, approaches a minimum and then rises again. This behavior may be explained by the mathematical relation $\sigma = \sigma_0 + \frac{\gamma_T}{2}(T - T_0)^2$. The rising surface tension at a greater temperature can lead to a fluid being drawn toward a hot surface, where there is a dry area, therefore improving boiling heat transfer. Since gradient in the concentration too gives rise to variation in surface tension, therefore a mathematical relation of the form: $\sigma = \sigma_0 + \frac{\gamma_T}{2}(T - T_0)^2 + \frac{\gamma_C}{2}(C - C_0)^2$, describes a self-rewetting fluid with thermal and solutal Marangoni convection. With such distinctive behavior, self-rewetting fluid finds applications in heat transfer devices such as heat

pipe, which is way more efficient than other traditional technics. Encouraged by the usefulness of self rewetting fluids, Abe and Iwasaki [28] conducted an experiment in microgravity region involving two adjacent vapour bubbles of self-wetting fluid and observed that thermocapillary action aided in the coalescence of two bubbles. Lim et al. [29] examined the thermo-capillary effect in the thin film flow of a fluid whose surface tension varies quadratically with temperature. Lin and Yang [30] studied the mass transfer Marangoni flow of a self re-wetting power-law fluid past a solid porous surface. As per their observation, power-law exponent reduces the shear stress as well as the velocity and concentration boundary layers. Kumari and Tripathi [31] performed a theoretical analysis on the movement of a fluid bubble through a self re-wetting fluid by considering both natural and Marangoni convections in the existence of a magnetic field. They observed that the flattening of the bubble can be curbed by intensifying magnetic field.

For surface tension driven flows over various geometries, researchers have either considered a linear surface tension- temperature and/or linear surface tension- concentration relation. However, the dependency of surface tension on temperature and/or concentration of non-linear nature has not been discussed yet, which actually corresponds to self-rewetting fluid. Also, as discussed above, presence of magnetic field is essential for controlling Marangoni convection, yet such an analysis is absent from the literature. Self-rewetting fluid are an important class of fluid which have many applications in heat transfer and also there are some applications of self-rewetting fluid in crystal growth in the reduced gravity environment. We observed that for such important kind of fluid, a detail study of the convection arising in reduced gravitational environment in the presence of external heat generating source under the influence of magnetic field have not been discussed previously. Through this article we aim to fill this gap. The research problem of this kind is very relevant in real life heat transfer instruments such as heat pipe, in which phase change in the form of vaporization and condensation is used to transfer heat from one point to other.

2 Mathematical Formulation

In this study, we consider a two dimensional, steady flow of a self re-wetting power-law fluid flowing over a circular surface, induced by thermal and solutal Marangoni convection. Permeation of the magnetic field along the transverse direction is also considered whereas the effect of induced magnetic field is not considered. A schematic of the considered problem is demonstrated in Figure 1, in which we have made use of cylindrical-polar coordinate. Following are the assumptions that have gone into modelling the flow situation:-

- The Marangoni convection appears at the inter-facial region of self re-wetting fluid, at $Z = H$, and the thickness of the fluid layer $H(t)$ is time-dependent, where H is denotes the thickness of the fluid in dimensional form.

- The temperature distribution at the disk surface is given as: $T' = T_0 + AR^{\frac{1}{2-n}}$ whereas the concentration distribution at the surface is given as: $C' = C_0 + AR^{\frac{1}{2-n}}$ of the disk surface.
- A magnetic field of variable nature: $B = B_0\sqrt{\frac{UR}{U_0R_0}}$ is permeating in the Z-direction.
- The energy balance equation is written in the consideration of heat source: $Q = Q_0\left(\frac{UR}{U_0R_0}\right)$.
- Surface tension-temperature-concentration relation is expressed as $\sigma = \sigma_0 + \frac{\gamma_T}{2}(T - T_0)^2 + \frac{\gamma_C}{2}(C - C_0)^2$, where $\gamma_T = \left.\frac{\partial^2\sigma}{\partial T'^2}\right|_{T'=T_0}$, $\gamma_C = \left.\frac{\partial^2\sigma}{\partial C^2}\right|_{C=C_0}$, and σ_0 are positive constants.

In accordance with the aforementioned assumptions, the partial differential equations for mass, momentum, and energy transfers of self re-wetting power-law liquid over the disk surface is given as follows:

$$\frac{\partial U}{\partial R} + \frac{U}{R} + \frac{\partial W}{\partial Z} = 0, \tag{1}$$

$$U\frac{\partial U}{\partial R} + W\frac{\partial U}{\partial Z} = \frac{\partial}{\partial Z}\left(\nu\left|\frac{\partial U}{\partial Z}\right|^{n-1}\frac{\partial U}{\partial Z}\right) - \frac{\chi B^2}{\rho}U, \tag{2}$$

$$U\frac{\partial T'}{\partial R} + W\frac{\partial T'}{\partial Z} = \frac{\partial}{\partial Z}\left(\alpha\left|\frac{\partial T'}{\partial Z}\right|^{n-1}\frac{\partial T'}{\partial Z}\right) + \frac{Q}{\rho c_p}\left(T' - T_0\right), \tag{3}$$

$$U\frac{\partial C'}{\partial R} + W\frac{\partial C'}{\partial Z} = \frac{\partial}{\partial Z}\left(\lambda\left|\frac{\partial C'}{\partial Z}\right|^{n-1}\frac{\partial C'}{\partial Z}\right). \tag{4}$$

The boundary conditions as per the assumptions are:

$$\text{at} \quad Z = 0: \;\; U = 0, \quad T' = T_0, \quad C' = C_0, \tag{5}$$

$$\text{at } Z = H: \;\; \nu\left|\frac{\partial U}{\partial Z}\right|^{n-1}\frac{\partial U}{\partial Z} = -\frac{\partial \sigma}{\partial R}, \;\; W = \frac{\partial H}{\partial t}, \;\; T' = T_0 + AR^{\frac{1}{2-n}}, \; C' = C_0 + AR^{\frac{1}{2-n}}. \tag{6}$$

In these equations, (U, W) represent velocity components in R and Z directions, temperature and species concentration are in dimensional form denoted as T' and C' respectively. Kinematic viscosity, mass diffusivity and thermal diffusivity are each expressed as $K_0 = \nu\left|\frac{\partial U}{\partial Z}\right|^{n-1}$, $K_2 = \lambda\left|\frac{\partial C'}{\partial Z}\right|^{n-1}$ and $K_1 = \alpha\left|\frac{\partial T'}{\partial Z}\right|^{n-1}$ respectively, where ν, λ and α are positive constants. In the above equation, σ represents the surface tension of a fluid, χ represents the electrical conductivity of fluid, ρ represents the density of a fluid, c_p represents the specific heat at constant pressure of fluid, A is a positive constant term and n represents the power-law index of a conducting fluid.

Equations 1 to 4 along with condition 5 and 6 are written in dimensional form. In order to convert these equations in non-dimensional form, following non-dimensional variables are used:

$$u = \frac{U}{U_0}, \;\; r = \frac{R}{R_0}, \;\; z = \frac{Z}{R_0}Re^{\frac{1}{n+1}}, \;\; w = \frac{W}{U_0}Re^{\frac{1}{n+1}}, \;\; C = \frac{C'}{C_0}, \;\; T = \frac{T'}{T_0}, \;\; h = \frac{H}{R_0}Re^{\frac{1}{n+1}}, \tag{7}$$

After incorporating Equation 7, governing Equations 1 to 4 are rewritten into dimensionless form, given below:

$$\frac{\partial u}{\partial r}+\frac{u}{r}+\frac{\partial w}{\partial z}=0, \tag{8}$$

$$u\frac{\partial u}{\partial r}+w\frac{\partial u}{\partial z}=\frac{\partial}{\partial z}\left(\left|\frac{\partial u}{\partial z}\right|^{n-1}\frac{\partial u}{\partial z}\right)-\frac{\chi B^2 R_0}{\rho U_0}u, \tag{9}$$

$$u\frac{\partial T}{\partial r}+w\frac{\partial T}{\partial z}=\frac{1}{Pr}\frac{\partial}{\partial z}\left(\left|\frac{\partial T}{\partial z}\right|^{n-1}\frac{\partial T}{\partial z}\right)+\frac{QR_0}{\rho c_p U_0}\left(T-1\right), \tag{10}$$

$$u\frac{\partial C}{\partial r}+w\frac{\partial C}{\partial z}=\frac{1}{Sc}\frac{\partial}{\partial z}\left(\left|\frac{\partial C}{\partial z}\right|^{n-1}\frac{\partial C}{\partial z}\right). \tag{11}$$

The non-dimensional form of boundary conditions are given as:

$$\text{at}\quad z=0:\ \ u=0,\quad C=1,\ \ T=1, \tag{12}$$

$$\text{at } z=h:\ \left|\frac{\partial u}{\partial z}\right|^{n-1}\frac{\partial u}{\partial z}=\frac{1}{n-2}\left[\frac{Ma_T}{Pr}+\frac{Ma_C}{Sc}\right]Re^{\frac{-3}{n+1}}r^{\frac{n}{2-n}},\ \ w=u\frac{\partial h}{\partial r}, \tag{13}$$

$$T=1+\frac{A}{T_0}R_0^{\frac{1}{2-n}}r^{\frac{1}{2-n}},\ \ C=1+\frac{A}{C_0}R_0^{\frac{1}{2-n}}r^{\frac{1}{2-n}},$$

where the dimensionless parameters $Re=\frac{U_0^{2-n}R_0^n}{\rho\nu}$, $Pr=\frac{\rho\nu}{\alpha U_0^{1-n}T_0^{n-1}}$ and $Sc=\frac{\rho\nu}{\lambda U_0^{1-n}C_0^{n-1}}$ are Reynolds number, Prandtl number and Schmidt number respectively. $M_a^C=\frac{\gamma_C A^2}{\lambda}\frac{R_0^{\frac{n}{2-n}+n}}{U_0C_0^{n-1}Re^{\frac{3-n}{n+1}}}$ and $M_a^T=\frac{\gamma_T A^2}{\alpha}\frac{R_0^{\frac{n}{2-n}+n}}{U_0T_0^{n-1}Re^{\frac{3-n}{n+1}}}$ represent the solutal and thermal Marangoni numbers respectively.

In order to solved partial differential Equations 8 to 11 along with conditions 12 and 13, we convert them into ordinary differential equations by using suitable similarity variables, which are given as:

$$\eta=C_2z,\ \ u=C_1r^{\frac{1}{2-n}}f'(\eta),\ \ \ w=-\frac{C_1}{C_2}\frac{3-n}{2-n}r^{\frac{n-1}{2-n}}f(\eta),\ \ T=1+\frac{A}{T_0}R_0^{\frac{1}{2-n}}r^{\frac{1}{2-n}}\theta(\eta),$$

$$C=1+\frac{A}{C_0}R_0^{\frac{1}{2-n}}r^{\frac{1}{2-n}}\phi(\eta),\ \ B^2=B_0^2C_1r^{\frac{n-1}{2-n}},\ \ Q=Q_0C_1r^{\frac{n-1}{2-n}},$$

where

$$C_1=\left(\frac{A}{C_0}R_0^{\frac{1}{2-n}}\right),\ C_2=\left(\frac{A}{C_0}R_0^{\frac{1}{2-n}}\right)^{\frac{2-n}{n+1}}.$$

After applying the similarity variables, governing Equations 8 to 11 are changed into following non-linear equations:

$$\left(\frac{1}{2-n}\right)f'^2-\left(\frac{3-n}{2-n}\right)ff''=\frac{\partial}{\partial\eta}\left(\left|f''\right|^{n-1}f''\right)-Mf', \tag{14}$$

$$\left(\frac{1}{2-n}\right) f'\theta - \left(\frac{3-n}{2-n}\right) f\theta' = \frac{1}{Pr}\frac{\partial}{\partial\eta}\left(\left|\theta'\right|^{n-1}\theta'\right) + Q^*\theta, \tag{15}$$

$$\left(\frac{1}{2-n}\right) f'\phi - \left(\frac{3-n}{2-n}\right) f\phi' = \frac{1}{Sc}\frac{\partial}{\partial\eta}\left(\left|\phi'\right|^{n-1}\phi'\right). \tag{16}$$

Converted boundary condition are given as:

$$\text{at} \quad \eta = 0: \quad f'(0) = 0, \quad \theta(0) = 0, \quad \phi(0) = 0, \tag{17}$$

$$\text{at} \quad \eta = \beta: \quad f''(\beta) = \left(M_a^T + M_a^c\right)^{\frac{1}{n}}, \quad f(\beta) = -C_2\left(\frac{2-n}{3-n}\right)\frac{\partial h}{\partial r} r f'(\beta), \quad \theta(\beta) = 1, \quad \phi(\beta) = 1, \tag{18}$$

where magnetic parameter is defined as $M = \frac{\chi B_0^2 R_0}{\rho U_0}$, heat generation or absorption coefficient is defined as $Q^* = \frac{Q_0 R_0}{\rho C_p U_0}$. The thermal and solutal Marangoni numbers M_a^T and M_a^c, are given as:

$$M_a^c = \frac{1}{n-2}\frac{Ma_C}{Sc} Re^{-\frac{3}{n+1}} \left(C_1 C_2\right)^{-n}, \tag{19}$$

$$M_a^T = \frac{1}{n-2}\frac{Ma_T}{Pr} Re^{-\frac{3}{n+1}} \left(C_1 C_2\right)^{-n}. \tag{20}$$

2.1 Quantities of physical interest

The Nusselt number Nu_r estimates the heat transfer rate and the Sherwood number Sh_r presents a measure of mass transfer rate at the disk surface. These two quantities are defined as follows:

$$Nu_r = \frac{r q_z}{K_1(T_0 - T_h)}, \tag{21}$$

$$Sh_r = \frac{r C_z}{K_2(C_0 - C_h)}, \tag{22}$$

where τ_z the radial shear stress, K_1 is the thermal diffusivity of the fluid, K_2 is mass diffusivity, q_z and C_z are the heat and mass transfer rates from the surface respectively, and they are given by

$$q_z = -K_1 \left.\frac{\partial T}{\partial z}\right|_{z=0}, \tag{23}$$

$$C_z = -K_2 \left.\frac{\partial C}{\partial z}\right|_{z=0}. \tag{24}$$

The dimensionless form of Nusselt number Nu and Sherwood number Sh are:

$$Nu = \frac{Nu_r}{C_2 r} = -\theta'(0), \tag{25}$$

$$Sh = \frac{Sh_r}{C_2 r} = -\phi'(0). \tag{26}$$

3 Solution Methodology

A numerical solution of system of Equation 14 to 16 constraint to conditions 17 and 18 can be obtained by bvp4c method. In order to make use of bvp4c method, the similarity expression for velocity, temperature and concentration are given in terms new set of variables $y_i, i = 1 : 7$, to define variables $f, f', f'', \theta, \theta', \phi$ and ϕ' and writing Equations 14 to 16 in the following form:

$$y_1' = y_2, \tag{27}$$

$$y_2' = y_3, \tag{28}$$

$$y_3' = \frac{1}{n|y_3|^{n-1}}\left(\frac{y_2^2}{2-n} + My_2 - \left(\frac{3-n}{2-n}\right)y_1y_3\right), \tag{29}$$

$$y_4' = y_5, \tag{30}$$

$$y_5' = \frac{\mathrm{Pr}}{n|y_5|^{n-1}}\left(\frac{y_2y_4}{2-n} - Q^*y_4 - \left(\frac{3-n}{2-n}\right)y_1y_5\right), \tag{31}$$

$$y_6' = y_7, \tag{32}$$

$$y_7' = \frac{Sc}{n|y_7|^{n-1}}\left(\frac{y_2y_6}{2-n} - \left(\frac{3-n}{2-n}\right)y_1y_7\right). \tag{33}$$

The above system is solved subject to conditions given in Equations 17 and 18, by taking initial guesses for each variable with the help of *bvp4c* routine of MATLAB.

4 Validation of numerical solution

To judge the precision of numerical method, we have realized an assessment for the numerical values of velocity $f(0)$ and concentration $\phi(0)$ with $M_a^T = 0$, $M_a^c = 0$ $M = 0$, $Q = 0$ against n and reversible boundary conditions at $\eta = 0$ and $\eta = \beta$ with those of Lin and Yang[30]. An excellent agreement is found between our result and that of Lin and Yang [30], which is shown in Table 1. This ensures that our numerical approach is trustworthy and that it may be utilized for the computation of further results.

5 Result and Discussion

On finding the solution of system of 1^{st}-order simultaneous Equations 27 to 33 subject to the conditions at the boundary in given Equations 17 to 18 using method explained above, results for velocity, temperature, concentration as well as quantities of physical interest i.e. Nusselt number Nu and Sherwood number Sh, are obtain and have been presented in Figures 2 to 15 along with the Tables 2 and 3. In these figures, the effect of pertinent flow parameters $M_a^T, M_a^C, M, Q, Pr, Sc$

and n, on velocity, temperature and concentration, are shown.

Figures 2 -4 show how magnetic field M affects velocity $f'(\eta)$, temperature $\theta(\eta)$ and concentration $\phi(\eta)$. It's seen that on increasing magnetic parameter M, the velocity of fluid decelerates, while the temperature and concentration of fluid increase. Such behavior of velocity, temperature, and concentration can be attributed to the property of magnetic field, which creates resistance to fluid velocity and generates a type of resistive force. Thus, intensifying magnetic field results in increased temperature and concentration. Figures 5 and 6 illustrate the influence of thermal Marangoni parameter M_a^T on velocity $f'(\eta)$ and temperature $\theta(\eta)$. In their study, the effect of thermal Marangoni parameter was exactly opposite to our finding in this research. Such an outcome is due to self re-wetting property of the fluid. Figures 7 and 8 show the impact of solutal Marangoni parameter M_a^c on velocity $f'(\eta)$ and concentration $\phi(\eta)$. When the solutal Marangoni parameter increases, velocity of fluid decreases, while the opposite is observed for concentration. Figure 9 illustrates the influence of heat source parameter Q on temperature $\theta(\eta)$. It is seen that increment in Q triggers a rise in temperature. Specifically, for an elevated value of Q, the heat source processes become more powerful, which leads to more heat entering the liquid and thus the higher temperature $\theta(\eta)$. Figure 10 illustrates the influence of Pr has on temperature $\theta(\eta)$.This graph demonstrates that as Pr is raised, temperature rises as well. Figure 11 illustrates the influence that power-law index n has on velocity $f'(\eta)$. We observe that an increase in the value of n form 0.4 to 0.8 results in a continuous decrement in the velocity. Since an increase in n strengthens the dimensionless shear stress, hence we observe a decrement in fluid velocity $f'(\eta)$ when n increases. Figure 12 illustrates the influence that Sc has on concentration $\phi(\eta)$. Upon increasing Schmidt number Sc, $\phi(\eta)$ increases. Basically, the value of concentration raises due to a reduction in mass dissipation.

Figure 13 illustrates the effect of thermal Marangoni number M_a^T on the velocity $f'(\eta)$ while neglecting the solutal Marangoni convection i.e. by taking $M_a^c = 0$. As the value of M_a^T increases, the fluid velocity decreases. In order to see the difference between effects of Marangoni parameters on pseudo-plastic fluid and that on dilatent fluid. We have drawn Figures 14 and 15. These figures illustrate the impact of thermal and solutal Marangoni number on temperature and concentration of dilatent fluid respectively. We see that increase in M_a^T leads to rise in temperature, whereas an increase in M_a^c tends to increase the concentration. On comparing Figures 6 and 14), we see that a peak in temperature of dilatent fluid is observed before the peak in temperature of pseudo-plastic fluid, also there is a more pronounced effect of thermal Marangoni parameter on dilatent fluid. A comparison of Figures 7 and 15 show that the effect of M_a^c on pseudo-plastic fluid is more pronounced then the effect of M_a^c on dilatent fluid.

The rates with which the transfer of heat and mass at the surface of disk take place, are given in terms of Nusselt number and Sherwood number respectively. Their estimates against different

parameter are shown in Tables 2 and 3. It is perceived from Table-2 that an elevation in the parameter M tends to diminish the Nusselt number. The magnetic field induces a force that reduces the fluid velocity, due to this intermolecular friction between fluid layers diminishes, so the heat transfer rate gets dropped and the Nusselt number decreases. We also observed that the thermal and solutal Marangoni parameters as well as the power-law index affect the Nusselt number adversely. This can be explain in the context of effect of Marangoni parameter on fluid velocity. It is observed from Figure 5 and Figure 7 that an increase in M_a^T and M_a^c reduces the fluid velocity and also, different layers move with varying velocities. This leads to an increase in the friction between different layers and as a result Nusselt number decreases. We see that when the value of parameters Pr and Q are increased, the Nusselt number decreases.

It's ascertained from Table-3 that an elevation in the parameter M tends to diminish the Sherwood number. It means that Sh is decreased by increasing the concentration of a fluid. We also observe that the solutal Marangoni parameters as well as the power-law index affect the Sherwood number adversely. Such effect of solutal Marangoni parameter on Sherwood number can be explain in the view of effect of M_a^c on concentration profile since increasing M_a^c result in increment of concentration profile through the boundary layer and this result in decreased concentration gradient and therefore, we observe reduced Sherwood number on increasing M_a^c.

6 Conclusions

For the purpose of this research, we examined the thermal and solutal Marangoni convection in the self-rewetting power-law fluid flowing over a disk surface, while a magnetic field pervade the concerned domain and heat source affects the thermal distribution. A summary of important findings based on results obtained can be found below:

- Intensifying magnetic field ramps-up the temperature and concentration of liquid, which in turn decelerates the fluid velocity.
- A rise in the rate of thermo-capillary convection tends to increase the temperature of a liquid whereas fluid velocity decelerates. Both the thermal and solutal Marangoni convections have noteworthy influence at the interfacial region. It shows positive impact on heat transfer rate due to which fluid velocity increases. Also on increasing the Marangoni parameters, thickness of fluid film reduces.
- The influence of both kind of convections at the interface affect the dilatant fluid and pseudo-plastic fluid differently. On enhancing the thermo-capillary convection, the temperature of Dilatant fluid shoots-up rather quickly as compared to pseudo-plastic fluid. However concentration of pseudo plastic fluid is more sensitive to solutal Marangoni convection than that of dilatant fluid.

- There is a smooth increment in the concentration of liquid when $n > 1$, whereas for $n = 1$, the increse in concentration is rather quick.

7 Future Work

- Researchers have not explored the unsteady induced magnetic field effect with hybrid nanofluids on a circular surface with nonlinear radiation parameters in the past, we would like to work on this.
- Researchers have not investigated the self-rewetting power law fluid with Arrhenius activation energy in the presence of induced magnetic field yet. We would like to carry out this work in the future.
- Researchers are yet to discuss the Soret and Dufour effects on a self-rewetting power law fluid flow over a circular disk with homogeneous and heterogeneous reaction.

References

[1] Sahu, A. K., Chhabra, R., and Eswaran, V., "Two-dimensional laminar flow of a power-law fluid across a confined square cylinder", *J. NonNewt. Fluid Mech.*, **165**(13-14), pp. 752-763 (2010).

[2] Kumar, A., Tripathi, R. and Singh, R. et al., "Simultaneous effects of nonlinear thermal radiation and joule heating on the flow of williamson nanofluid with entropy generation", *Phys. A: Stat. Mech.*, **551**, pp. 123972 (2020).

[3] Hussain, S. M. and Jamshed, W., "A comparative entropy based analysis of tangent hyperbolic hybrid nanofluid flow: Implementing finite difference method"; *Int. Commun. Heat Mass Transf.* , **129**, pp. 105671 (2021).

[4] Kumar, A., Singh, R., and Sheremet, M. A., "Analysis and modeling of magnetic dipole for the radiative flow of non-newtonian nanomaterial with arrhenius activation energy", *Math. Methods Appl. Sci*, https://doi.org/10.1002/mma.7124 (2021).

[5] Wang, S. and Yu, B., " Analysis of seepage for power-law fluids in the fractal-like tree network", *Tranp. Porous Media*, **87**(1), pp. 191-206 (2011).

[6] Nitin, S. and Chhabra, R.," Sedimentation of a circular disk in power law fluids", *J. Colloid Interface Sci.*, **295**(2), pp. 520-527 (2006).

[7] Bharti, R. P., Sivakumar, P., and Chhabra, R., "Forced convection heat transfer from an elliptical cylinder to power-law fluids". *Int. J. Heat Mass Transf.*, **51**(7-8), pp. 1838-1853 (2008).

[8] Ming, C., Zheng, L., and Zhang, X., " Steady flow and heat transfer of the power-law fluid over a rotating disk", *Int. Comm. Heat Mass Transf.*, **38**(3), pp. 280284,(2011).

[9] Li, B., Zheng, L., and Zhang, X.," Comparison between thermal conductivity models on heat transfer in power-law non-newtonian fluids", *J. Heat Transf.*, **134**(4), pp.041702 (2012).

[10] Lin, Y. and Jiang, Y.," Effects of brownian motion and thermophoresis on nanofluids in a rotating circular groove: A numerical simulation", *Int. J. Heat Mass Transf.*, **123**, pp. 569-582 (2018).

[11] Gaffar, S. A., Prasad, V. R. and Reddy et al., "Radiative flow of third grade non-newtonian fluid from a horizontal circular cylinder", *Nonlinear Eng.*, **8**(1), pp. 673687 (2019).

[12] Sadiq, M. A. and Hayat, T., " Entropy optimized flow of reiner-rivlin nanofluid with chemical reaction subject to stretchable rotating disk", *Alexandria Eng. J.* **61**(5), pp. 3501–3510 (2021).

[13] Napolitano, L. "Surface and buoyancy driven free convection". *Acta Astronautica*, **9**(4), pp. 199215 (1982).

[14] Boeck, T. and Thess, A., "Power-law scaling in benard-marangoni convection at large prandtl numbers", *Phy. Review E.*, **64**(2), pp. 027303(2001).

[15] Lin, Y. and Zheng, L., "Marangoni boundary layer flow and heat transfer of copper-water nanofluid over a porous medium disk", *AIP Advances*,**5**(10) pp. 107225 (2015).

[16] Gupta, A. and Surya, D., "Convection in a thin liquid layer with mixed thermal boundary conditions: B'enardmarangoni convection", *Proc. Natl. Acad. Sci. India - Phys. Sci.*, **88**(1), pp. 73-79 (2018).

[17] Kumari, A. and Tripathi, R., " Irreversibility analysis of thermo-solutal Marangoni convection in Maxwell power-law-fluid flow",*Math. Methods Appl. Sci.*, https://doi.org/10.1002/mma.9065, (2023).

[18] Jin, K., Kumar, P. and Vanka, S. et al.,"Rise of an argon bubble in liquid steel in the presence of a transverse magnetic field", *Phys. Fluids.*, **28**(9), pp. 093301 (2016).

[19] Wilson, S., "The effect of a uniform magnetic field on the onset of steady marangoni convection in a layer of conducting fluid with a prescribed heat flux at its lower boundary", *Phys. Fluids.*, **6**(11), pp. 3591-3600 (1994).

[20] Magyari, E. and Chamkha, A., " Exact analytical results for the thermosolutal mhd marangoni boundary layers", *Int. J. Therm. Sci.*, **47**(7), pp. 848857 (2008).

[21] Abel, M. S., Datti, P. S., and Mahesha, N., " Flow and heat transfer in a power-law fluid over a stretching sheet with variable thermal conductivity and non-uniform heat source", *Int. J. Heat Mass Transf.*, **52**, (11-12), pp. 2902-2913 (2009).

[22] Jiao, C., Zheng, L., and Ma, L. , "MHD thermosolutal marangoni convection heat and mass transport of power law fluid driven by temperature and concentration gradient", *AIP Advances*, **5**(8), pp. 087160(2015).

[23] Jawad, M., Saeed, A. and Gul, T., et al.," Unsteady thermal maxwell power law nanofluid flow subject to forced thermal marangoni convection", *Sci. Rep.*, **11**(1), pp. 1-14 (2021).

[24] Nandi, S. and Kumbhakar, B.," Viscous dissipation and chemical reaction effects on tangent hyperbolic nanofluid flow past a stretching wedge with convective heating and naviers slip conditions", *Iran. J. Sci. Technol. - Trans. Mech. Eng.*,**46**(2), pp.379–397 (2021).

[25] Tripathi, R., " Marangoni convection in the transient flow of hybrid nanoliquid thin film over a radially stretching disk", *P. I. Mech. Eng. E.J. Pro.*, **235**(4) pp. 800–811 (2021).

[26] Hussain, S. M.," Dynamics of radiative williamson hybrid nanofluid with entropy generation: significance in solar aircraft", *Sci. Rep.*, **12**(1), pp. 123 (2022a)

[27] Abbas, N., Shatanawi, W., and Shatnawi, T. AM.,"Transportation of nanomaterial Maxwell fluid flow with thermal slip under the effect of Soret–Dufour and second-order slips: nonlinear stretching, *Sci. Reports*, **13**(1), pp. 2182, (2023).

[28] Abe, Y. and Iwasaki, A., "Microgravity experiments on dual vapor bubbles of self-wetting fluid", *AIP conf. proce.* **608**(1), pp.189-196 (2002).

[29] Lim, E., Kueh, T. C., and Hung, Y. M.,"Inverse-thermocapillary evaporation in a thin liquid film of self-rewetting fluid", *Int. J. Num. Method. H.*, **31**(4), pp. 1124–1143.(2020).

[30] Lin, Y. and Yang, M., " Marangoni flow and mass transfer of power-law non-newtonian fluids over a disk with suction and injection", *Commun. Theor. Phys.*, **72**(9), pp.095003, (2020).

[31] Kumari, A. and Tripathi, R., " Rise of a bubble through a self-rewetting fluid under the combined influence of gravity-driven convection and marangoni convection. Proceedings of the Institution of Mechanical Engineers", *P. I. Mech. Eng. E.J. Pro*, **236**(3), pp.814–823 (2022).

Apendix-(i)

Fig. No.	Figure Caption
Figure 1	Geometry of the problem
Figure 2	This graph illustrates the relationship between velocity $f'(\eta)$ and magnetic parameter M.
Figure 3	This graph illustrates the relationship between temperature $\theta(\eta)$ and magnetic parameter M.
Figure 4	This graph illustrates the relationship between concentration $\phi(\eta)$ and Magnetic parameter M
Figure 5	This graph illustrates the relationship between velocity $f'(\eta)$ and Thermal Marangoni parameter M_a^T.
Figure 6	This graph illustrates the relationship between temprature $\theta(\eta)$ and Thermal Marangoni parameter M_a^T.
Figure 7	This graph illustrates the relationship between velocity $f'(\eta)$ and Solutal Marangoni parameter M_a^c.
Figure 8	This graph illustrates the relationship between concentration $\phi(\eta)$ and Solutal Marangoni parameter M_a^c.
Figure 9	This graph illustrates the relationship between temperature $\theta(\eta)$ and heat source parameter Q.
Figure 10	This graph illustrates the relationship between temperature $\theta(\eta)$ and Prandtl number Pr
Figure 11	This graph illustrates the relationship between velocity $f'(\eta)$ and power-law index number n.
Figure 12	This graph illustrates the relationship between concentration $\phi(\eta)$ and Schmidt number Sc
Figure 13	This graph illustrates the relationship between velocity $f'(\eta)$ and Thermal Marangoni parameter M_a^T.
Figure 14	This graph illustrates the relationship between temprature $\theta(\eta)$ and Thermal Marangoni parameter M_a^T.
Figure 15	This graph illustrates the relationship between concentration $\phi(\eta)$ and Solutal Marangoni parameter M_a^c.
Table 1	Comparison of values of $f(0)$ and $\phi(0)$ for various values of n with published results for $M_a^T = 0$, $M_a^c = 0$, $M = 0$, $Q = 0$ with reversible boundary conditions
Table 2	Nusselt number Nu for distinct parameters
Table 3	Sherwood number Sh for distinct parameters

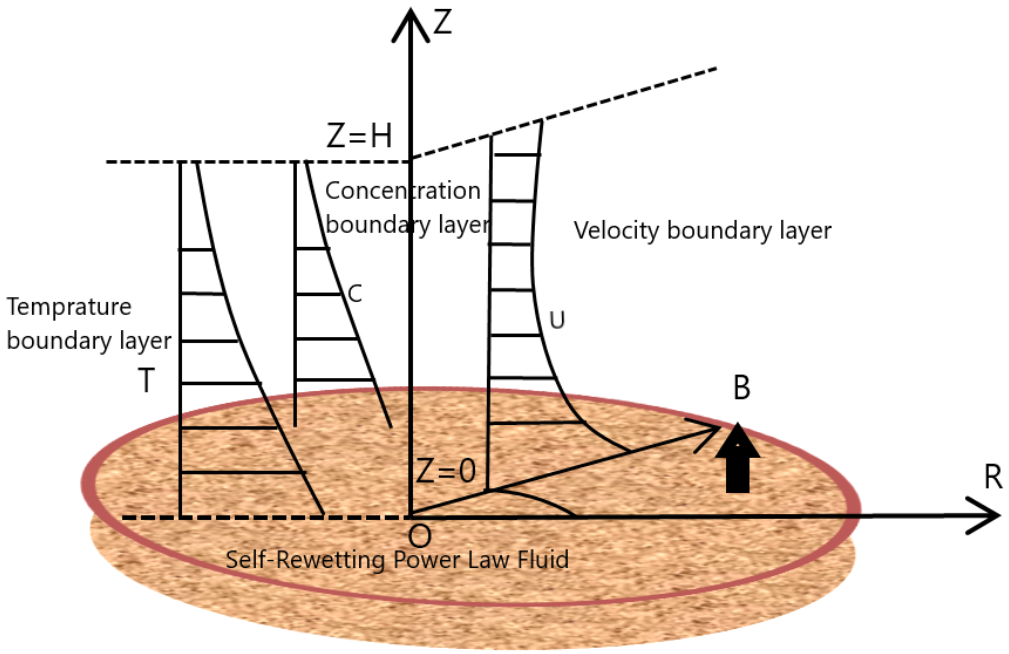

Figure 1: Geometry of the problem

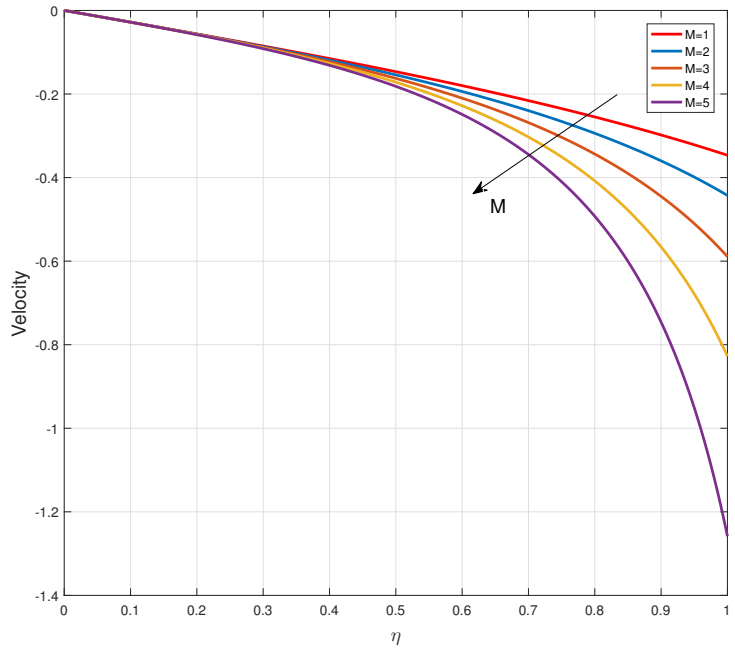

Figure 2: This graph illustrates the relationship between velocity $f'(\eta)$ and magnetic parameter M.

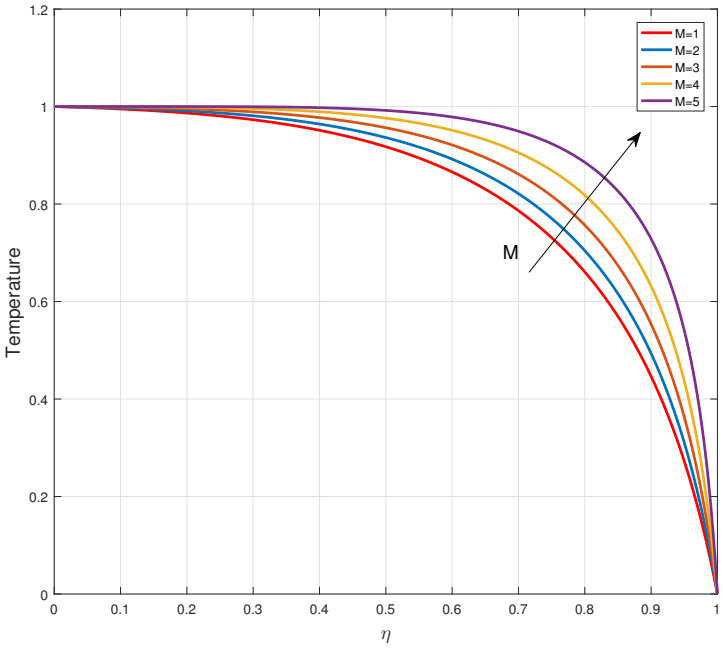

Figure 3: This graph illustrates the relationship between temperature $\theta(\eta)$ and magnetic parameter M.

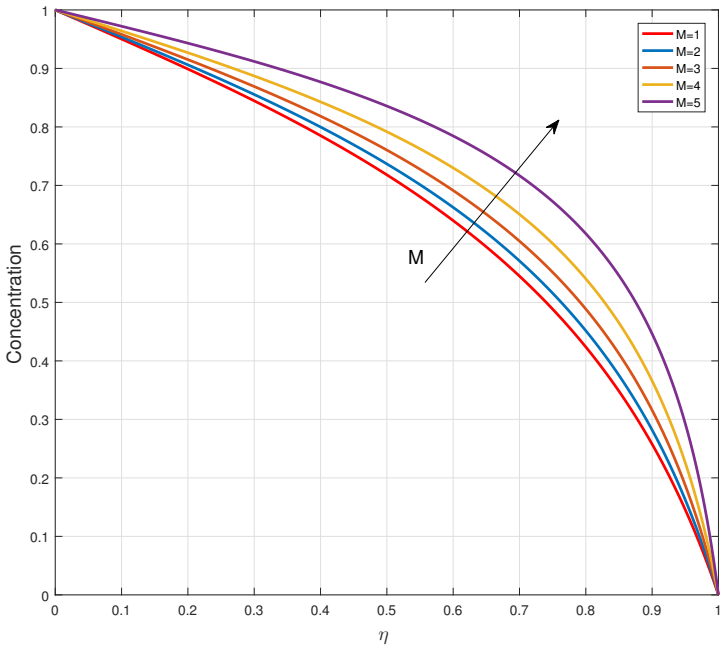

Figure 4: This graph illustrates the relationship between concentration $\phi(\eta)$ and Magnetic parameter M.

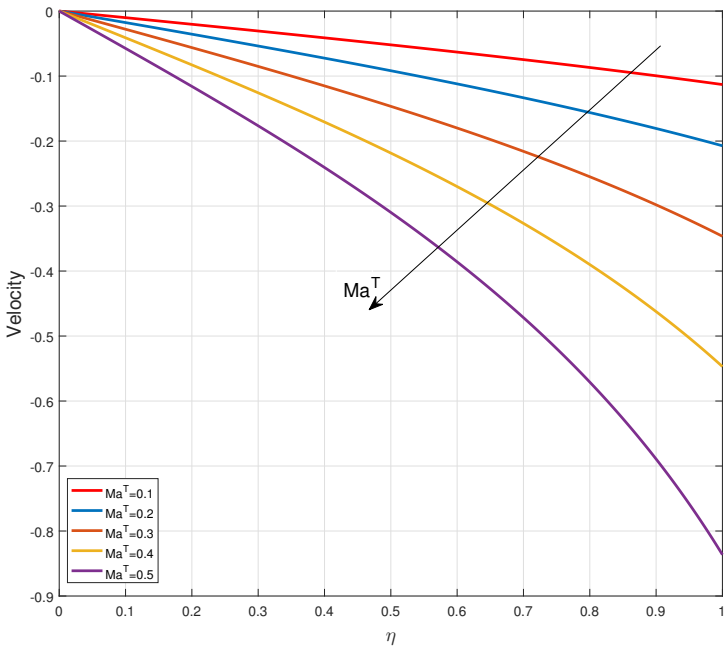

Figure 5: This graph illustrates the relationship between velocity $f'(\eta)$ and Thermal Marangoni parameter M_a^T.

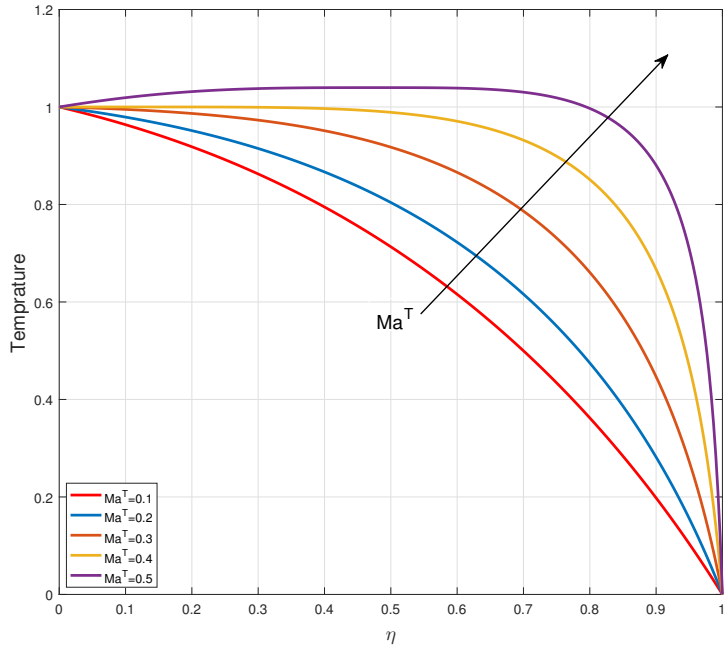

Figure 6: This graph illustrates the relationship between temprature $\theta(\eta)$ and Thermal Marangoni parameter M_a^T.

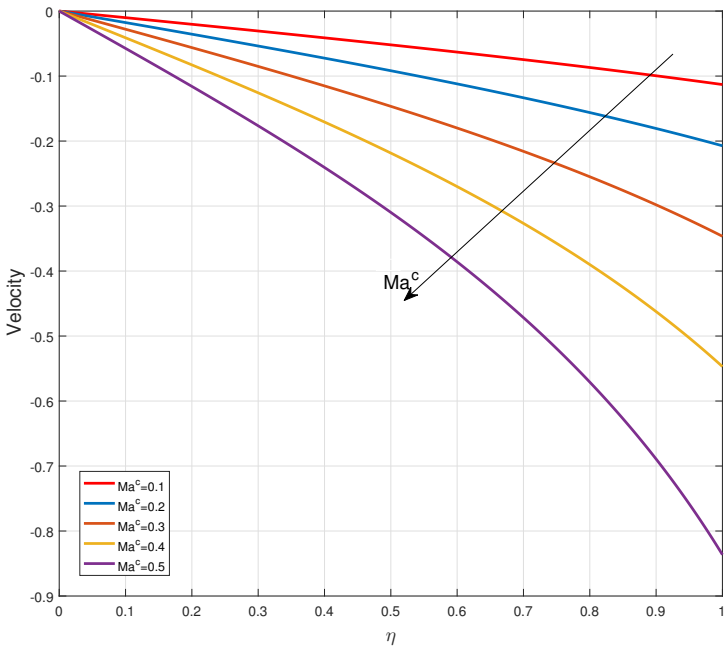

Figure 7: This graph illustrates the relationship between velocity $f'(\eta)$ and Solutal Marangoni parameter M_a^c.

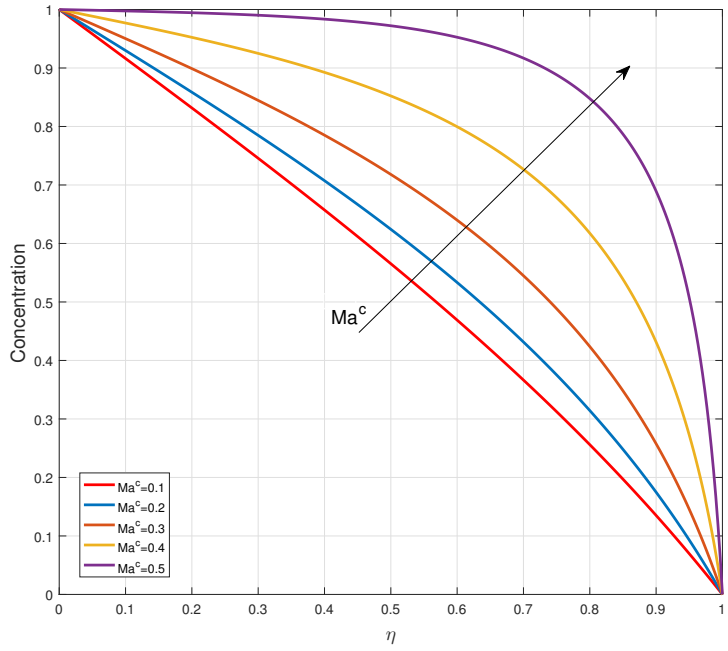

Figure 8: This graph illustrates the relationship between concentration $\phi(\eta)$ and Solutal Marangoni parameter M_a^c.

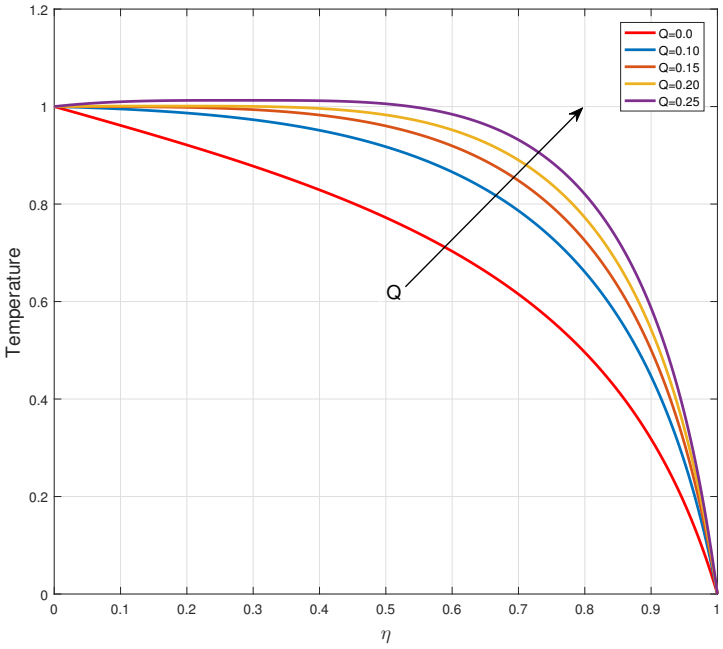

Figure 9: This graph illustrates the relationship between temperature $\theta(\eta)$ and heat source parameter Q.

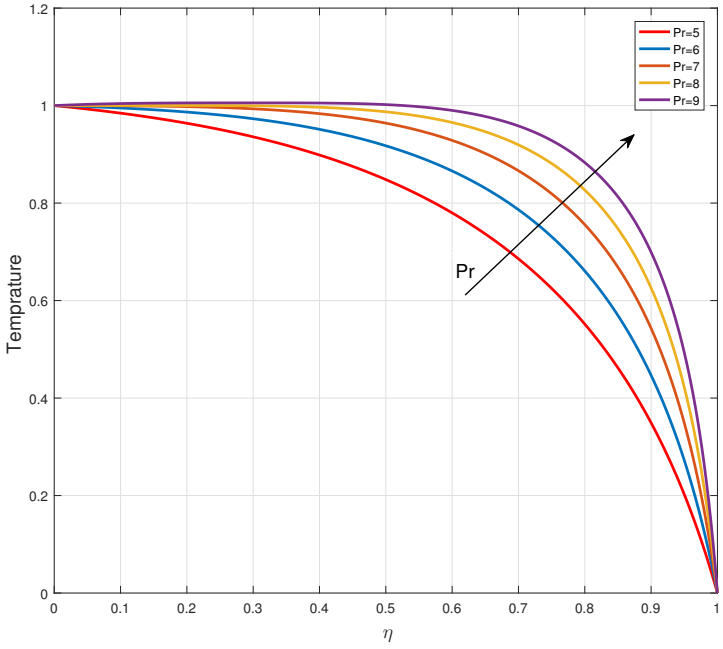

Figure 10: This graph illustrates the relationship between temperature $\theta(\eta)$ and Prandtl number Pr.

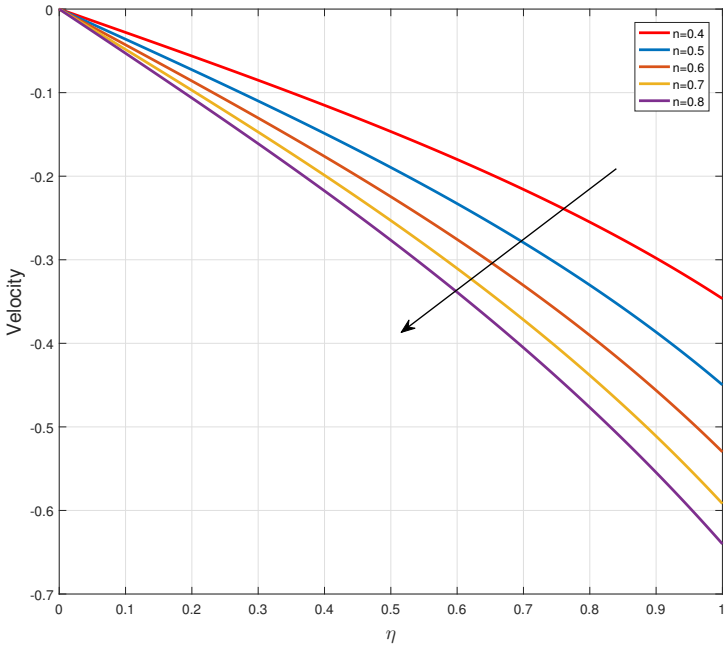

Figure 11: This graph illustrates the relationship between velocity $f'(\eta)$ and power-law index number n.

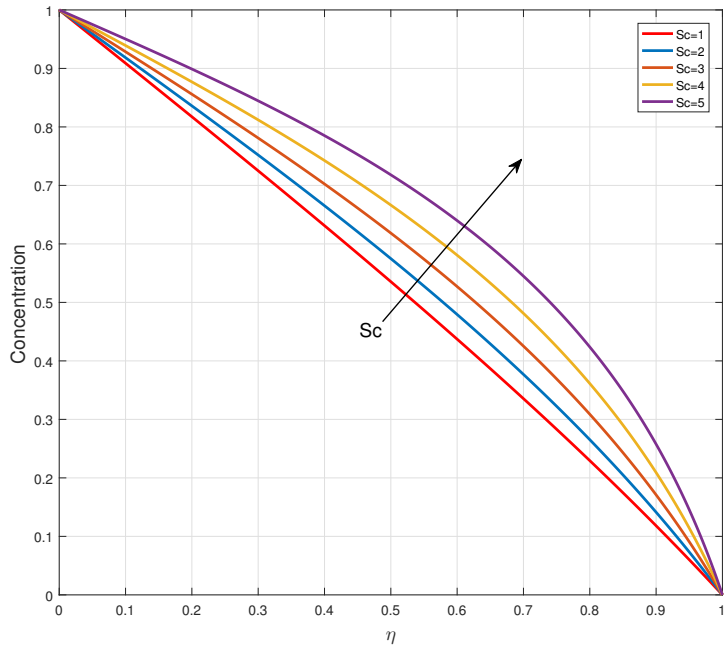

Figure 12: This graph illustrates the relationship between concentration $\phi(\eta)$ and Schmidt number Sc.

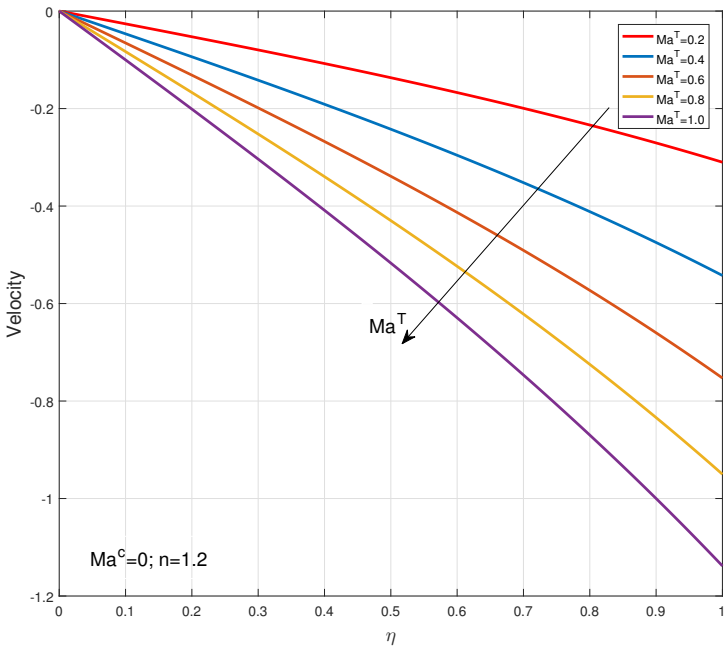

Figure 13: This graph illustrates the relationship between velocity $f'(\eta)$ and Thermal Marangoni parameter M_a^T.

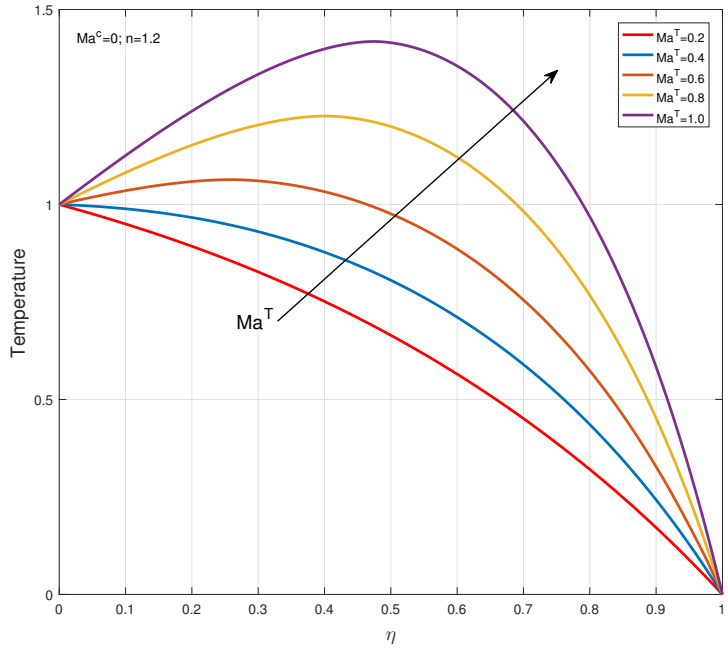

Figure 14: This graph illustrates the relationship between temprature $\theta(\eta)$ and Thermal Marangoni parameter M_a^T.

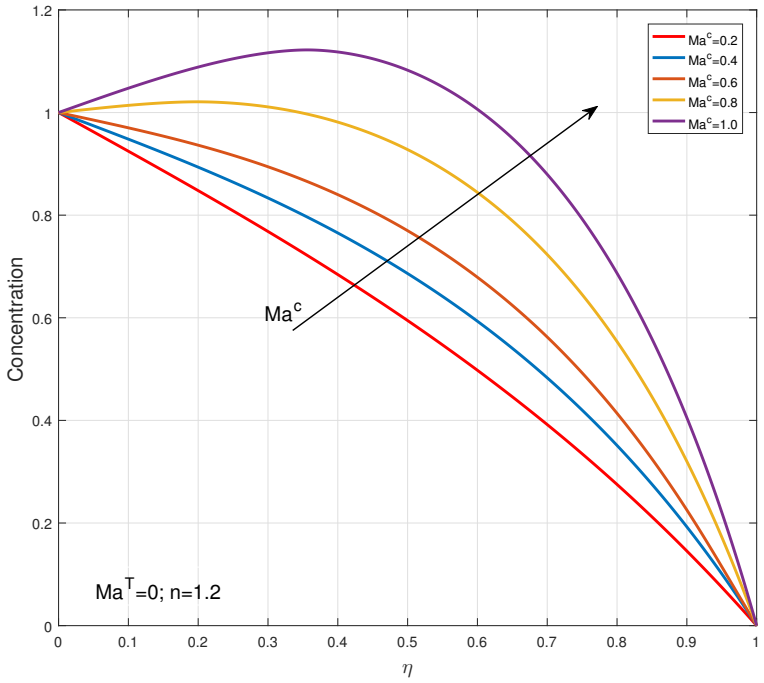

Figure 15: This graph illustrates the relationship between concentration $\phi(\eta)$ and Solutal Marangoni parameter M_a^c.

Table 1: Comparison of values of $f(0)$ and $\phi(0)$ for various values of n with published results for $M_a^T = 0$, $M_a^c = 0$, $M = 0$, $Q = 0$ with reversible boundary conditions

Power Law index n	Lin and Yang $f(0)$	Present paper for velocity	Lin and Yang $\phi(0)$	Present paper for concentration
0.3	0.631403	0.631429	0.936506	0.936509
0.5	0.621587	0.621585	0.919006	0.919008
0.7	0.611383	0.611378	0.899606	0.899627
1.0	0.566154	0.566109	0.881908	0.881987

Table 2: Nusselt number Nu for distinct parameters

M	M_a^T	M_a^c	n	Pr	Q	$-\theta'(0)$
1						0.0371
2						0.0215
3	0.3	0.3	0.4	6	0.1	0.0083
	0.1					0.3229
	0.2					0.1784
1	0.3	0.3	0.4	6	0.1	0.0371
		0.1				0.3229
		0.2				0.1784
1	0.3	0.3	0.4	6	0.1	0.0371
			0.4			0.0371
			0.5			0.0252
1	0.3	0.3	0.6	6	0.1	0.0133
				5		0.1345
				6		0.0371
1	0.3	0.3	0.4	7	0.1	0.0015
					0	0.3840
					0.1	0.0371
1	0.3	0.3	0.4	6	0.2	0.0002

Table 3: Sherwood number Sh for distinct parameters

M	M_a^T	M_a^c	n	Sc	$-\phi'(0)$
1					0.4954
2					0.4602
3	0.3	0.3	0.4	5	0.4158
	0.1				0.8366
	0.2				0.6995
1	0.3	0.3	0.4	5	0.4954
		0.1			0.8366
		0.2			0.6995
1	0.3	0.3	0.4	5	0.4954
			0.4		0.4954
			0.5		0.4469
1	0.3	0.3	0.6	5	0.4206
				1	0.9102
				2	0.8146
1	0.3	0.3	0.4	3	0.7131

Apendix-(ii)

Nomenclature			
	Dimensional forms		**Non-Dimensional forms**
R,Z	Radial and Transverse direction, m	r,z	Radial and Transverse direction
U,W	Velocity component in radial and transverse direction, m/s	u,w	Velocity component in radial and transverse direction
T'	Temperature K	T	Temperature
C'	Concentration	C	Concentration
Q	Heat generation/absorption parameter	Q^*	Heat generation/absorption parameter
H	Fluid thickness, m	h	Fluid thickness
MHD	Magnetohydrodynamics	2-D	Two dimensional
R_0, Q_0	Positive constant	T_0	Temperature at the disk surface
n	Power-law index	t	Time, s
Greek Symbols			
Re	Reynolds number	ν	Kinematic viscosity, m^2/s
Sh_r	Sherwood number	M	Magnetic parameter
Pr	Prandtl number	σ	Surface tension, m/s^2
τ_z	Shear stress of the fluid, Pa	q_z	Surface heat flux, W/m^2
λ	Magnetic Prandtl number	σ_0	Initial surface tension
M_a^T	Thermal Marangoni number	χ	Electrical conductivity
M_a^C	Solutal Marangoni number	B_0	applied magnetic field
c_f	Skin friction coefficent,	N_u	Nusselt number
γ_T,γ_C	surface tension coefficients for temperature and concentration	β	Film thickness
μ_e	Magnetic diffusivity	ρ	Density of the fluid, kg/m^3
α	Thermal diffusivity, m^2/s	K	Flow consistency index
c_p	Specific heat at constant pressure, $J/(kgK)$	K_0, K_1, K_2	Positive constant

Authors

Vineet Kumar Chaurasiya is a PhD student in the Department of Mathematics at National Institute of Technology, Jamshedpur-831014, Jharkhand, India. Email-id:- 1990.vineet.1990@gmail.com, Phone no. +919451227863. He received his M.Sc degree from Indian Institute of Technology Kharagpur. His research interests include Newtonian and Non-Newtonian Fluids, Marangoni convection, Thin-film flow, nanomaterials, hybrid nanomaterials, heat and mass transfer.

Rajat Tripathi is Assistant Professor in the Department of Mathematics at National Institute of Technology, Jamshedpur-831014, Jharkhand, India.Email-id:- rtripathi.math@nitjsr.ac.in, Phone no. +917909067450. He is a member of the Society of Applied Mathematics (SAM), research group. His areas of interest include Thin Film Flows, Magnetohydrodynamics, Heat, Mass Transfer, Boundary Layer Theory flow problems in nanosystems.

Ramayan Singh is Associate Professor in the Department of Mathematics at National Institute of Technology, Jamshedpur-831014, Jharkhand, India.Email-id:- rsinghmath@nitjsr.ac.in, Phone no. +919430304200. He is a member of the Society of Applied Mathematics, research group. His research interests include theoretical fluid flow modeling along stretching surfaces, Nanofluid flows, and flow along curved surfaces.